ELSEVIER

Contents lists available at ScienceDirect

Journal of Membrane Science Letters

journal homepage: www.elsevier.com/locate/memlet



Sustainable nanofiltration membranes based on biosourced fully recyclable polyesters and green solvents



Rifan Hardian^a, Robin M. Cywar^b, Eugene Y.-X. Chen^b, Gyorgy Szekely^{a,*}

- ^a Advanced Membranes and Porous Materials Center, Physical Science and Engineering Division, King Abdullah University of Science and Technology (KAUST), Thuwal 23955-6900, Saudi Arabia
- ^b Department of Chemistry, Colorado State University, Fort Collins, CO 80523-1872, USA

ARTICLE INFO

Keywords: Nanofiltration Polyester Green solvent Polarclean Biomaterial

ABSTRACT

Herein, we report a new class of biosourced nanofiltration membranes based on chemically recyclable aliphatic polyesters (P(4,5-T6GBL)) and the use of green solvents. Given their chemical recyclability and potential biodegradability, these polyester membranes were designed to have a sustainable lifecycle. The effect of membrane thickness and solvent/non-solvent diffusivity on membrane morphology and organic solvent nanofiltration were investigated. Long-term membrane stability was tested in a continuous crow-flow filtration rig over a week, which exhibited stable methanol permeance at 8.6 ± 0.1 L m⁻² h⁻¹ bar⁻¹. The rejection profiles of the pharmaceuticals oleuropein (540 g mol⁻¹) and roxithromycin (837 g mol⁻¹) were also found to be stable at 87% and 100%, respectively.

1. Introduction

Membrane technology offers greater energy-efficient separation compared to conventional thermal processes. Environmental awareness is driving membrane development toward more sustainable cradle-tograve approaches. All aspects, including the source of raw materials, polymer synthesis, material fabrication, solvent selection, and end-oflife membrane recyclability, must be considered. The development of chemically recyclable polymers promises a closed-loop approach toward a circular plastic economy (Zhu et al., 2018; Zhu and Chen, 2018). Moreover, selecting renewable or naturally-derived raw material sources is encouraged to ensure sustainability and minimize the use of nonrenewable petrochemical-based materials. The use of organocatalysts to substitute metal-based catalysts for polymerization/depolymerization is highly desirable (Cywar et al., 2019). From an energy-saving perspective, ambient-condition polymer synthesis processes are highly sought after. Furthermore, as membrane fabrication relies on solution processability, the sustainability of membrane fabrication is also determined by the use of green solvents as alternatives to common toxic solvents (Figoli et al., 2014; Kim and Nunes, 2021). Commonly used solvents in membrane fabrication, such as N-methylpyrrolidone, N,Ndimethylformamide, N,N-dimethylacetamide, are known to be toxic, harmful, and derived from non-renewable resources. The replacement of these solvents with greener alternatives promotes environmental conservation and good health, which are in line with the United Nations

Organic solvent nanofiltration (OSN) membranes offer numerous advantages for various industrial sectors. In particular, OSN offers a sustainable solution for the purification and concentration of high-value fine chemicals and pharmaceuticals compared to conventional thermal-based separation technologies (Goh et al., 2021). Other applications of OSN include solvent recovery and separations for petrochemicals and dyes (Marchetti et al., 2014). Although research on the sustainable fabrication of OSN membranes has rapidly emerged over recent years (Xie et al., 2021), sustainable OSN membrane lifecycles have not been realized. The need for end-of-life of OSN membranes requires fully recyclable materials, which triggered the current research.

Herein, we synthesized linear polyesters that can be derived from natural sources and prepared via sustainable organocatalysis and fabricated nanofiltration membranes in green solvents. The polymer was obtained through the efficient organocatalytic ring-opening polymerization (ROP) reaction of 4,5-*trans*-cyclohexyl-fused γ -butyrolactone (4,5-T6GBL) at room temperature (Cywar et al., 2019). The replacement of conventional metal-based catalysts with organocatalysts enables metal-residue-free polymer membranes and applications, including for the electronic, biomedical, pharmaceutical, and food processing/packaging

E-mail address: gyorgy.szekely@kaust.edu.sa (G. Szekely). URL: https://www.szekelygroup.com (G. Szekely)

Sustainable Development Goals. The need for employing green solvents, particularly in polymer membrane fabrication, has been highlighted in recent publications (Hessel et al., 2022; Xie et al., 2021; Zou et al., 2021). PolarClean is one of the promising green solvents to replace polar aprotic solvents in the preparation of polymer dope solutions (Cseri and Szekely, 2019; Wang et al., 2019; Xie et al., 2020).

^{*} Correspondence author.

fields (Cywar et al., 2019). The monomer γ -butyrolactone (GBL) can be synthesized from succinic acid, which is a biomass derivative (Caretto et al., 2014). However, the polymerization of GBL is impractical because it occurs at subzero temperatures and possesses limited thermostability (Hong and Chen, 2016). Fusing an additional ring (*trans*-cyclohexane) at the β , γ - or 4,5-position of the GBL ring (i.e., 4,5-T6GBL) has been reported to enhance ring strain, which enables the polymerization reaction to occur at room temperature and increases the resulting polymer's thermostability (Cywar et al., 2019). In this work, 4,5-T6GBL, as the building block (monomer) of a P(4,5-T6GBL) polymer, was synthesized from diethyl malonate and cyclohexene oxide (Scheme S1), chemicals that can be sourced from biomass (Jagatić Korenika et al., 2020; Winkler et al., 2014).

2. Experimental section

2.1. Polymer P(4,5-T6GBL) synthesis

The polymer synthesis followed the reported literature (Cywar et al., 2019). 0.571 mmol of catalysts (Diisopropylthiourea/DiiPrTU) and 0.571 mmol of co-catalyst (1,3-dimesitylimidazol-2-ylidene/IMes) were dissolved in 57.1 mmol monomer (4,5-T6GBL/M) in an oversized glass jar, followed by the injection of 0.0286 mmol initiator (Benzyl alcohol/BnOH) via glass syringe. The molar ratio of the constituents is [M]/[DiiPrTU]/[IMes]/[BnOH] = 2000/20/20/1.

2.2. Membrane fabrication

700 mg of PolarClean solvent (Solvay) was added to 300 mg of P(4,5-T6GBL) polymer to make 30% polymer dope solution. Homogeneous P(4,5-T6GBL) dope solutions were realized by overhead stirring the components at 50 rpm at room temperature for 20 h. Then, degassing was performed under a nitrogen atmosphere in an incubator shaker at 200 rpm and at 25 °C for 4 h to ensure that the dope solution was free from any entrapped gas. The membranes were cast onto a Novatex 2471 non-woven polypropylene support using an Elcometer 4340 film applicator with a casting knife. M1 was cast by using 250 μ m thickness and the film was immediately immersed in a water coagulation bath at room temperature (23 °C) for 24 h. M2 was prepared following the same procedure as M1, but the casting knife was set to 150 μ m. M3 was fabricated using 150 μ m casting knife thickness and the film was subsequently immersed in a 60 °C water coagulation bath and let to cool down to room temperature for 24 h.

2.3. Nanofiltration tests

A cross-flow nanofiltration skid having three membrane cells with an active area of $6.25~\rm cm^2$, a back pressure regulator, a high-pressure pump and a microannular gear pump was used for membrane separation. The flow rate of the microannular gear pump was maintained at a constant rate of $100~\rm L~h^{-1}$ to minimize concentration polarization. The membranes were conditioned in a solvent–solute mixture at 30 bar for 24 h prior to taking permeate and retentate samples for the rejection determination. The volume of the solvent permeating through the membrane (V) at a certain time (t) over the active membrane surface area (A) was used to calculate the flux. The reported membrane performance values are the average values of three independently prepared membranes.

3. Results and discussion

The structural transformation of 4,5-T6GBL into P(4,5-T6GBL) and its sustainable lifecycle, including membrane fabrication and depolymerization, are shown in Fig. 1a. The characteristics of cyclohexane aliphatic CH_2 stretching are clearly visible in the Fourier transform

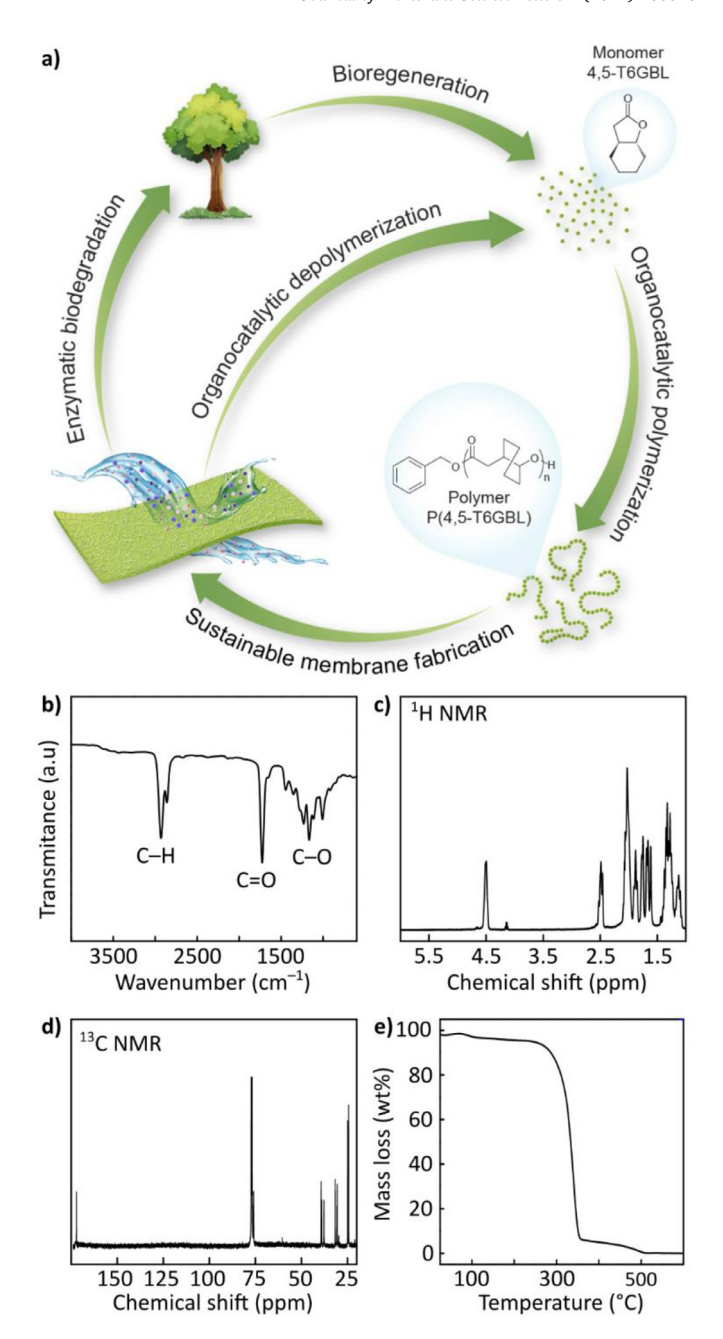


Fig. 1. (a) Sustainable lifecycle of polyester-based membranes. FTIR (b), $^1{\rm H}$ NMR (c), $^{13}{\rm C}$ NMR spectra (d), and (e) TGA profile of P(4,5-T6GBL).

infrared (FTIR) spectrum at $2861-2931 \, \mathrm{cm}^{-1}$ (Fig. 1b). Typical asymmetric C=O stretching and C-O vibrations were also observed at $1728 \, \mathrm{and} \, 1165 \, \mathrm{cm}^{-1}$, respectively, which indicated the successful synthesis of P(4,5-T6GBL). Herein, we used organic dual catalysis with an *N*-heterocyclic carbene, 1,3-dimesitylimidazol-2-ylidene (IMes), and diisopropylthiourea (DiⁱPrTU) with a benzyl alcohol (BnOH) initiator at a 4,5-T6GBL:DiⁱPrTU:IMes:BnOH ratio of 2000:20:20:1 to produce linear P(4,5-T6GBL) for membrane preparation (Scheme S2) (Cywar et al., 2019). Catalysis is highlighted as one of the 12 principles of green chemistry. In particular, organocatalysis is considered a greener approach to traditional metal-based catalysis because it does not require the use of toxic and often precious metals (McKeown et al., 2020). Our catalytic system can be considered more sustainable than metal-based catalysts (Table S10). The synthesized polymer had a number-average molecular weight (M_n) of 85.1 kDa and a dispersity index (P) of 1.08, as

determined through gel permeation chromatography in CHCl₃. Owing to its relatively high molecular weight, the $^1\mathrm{H}$ and $^{13}\mathrm{C}$ NMR spectra (Fig. 1c and d) of the linear P(4,5-T6GBL) did not exhibit characteristic end-group peaks at 5.1 and 128 ppm, respectively. A detailed assignment of the NMR peaks were provided in Figs. S4–S5. The polymer exhibited good thermal stability with a degradation temperature ($T_{\rm d}$) of 317 $^{\circ}\mathrm{C}$ (Fig. 1e) and a glass transition temperature ($T_{\rm g}$) of 72.7 $^{\circ}\mathrm{C}$ (Fig. S3), which is similar to the previously reported $T_{\rm g}$ value of 74 $^{\circ}\mathrm{C}$ (Cywar et al., 2019).

P(4,5-T6GBL) is chemically recyclable, which allows for the complete recovery of a pure building block via depolymerization, thus providing a viable solution for the end-of-use issue of polymer membranes and offering a closed-loop strategy toward a circular polymer economy (Zhu and Chen, 2018). We have demonstrated the recyclability of the membrane via its depolymerization into monomers. A metal-free and therefore sustainable organocatalytic reaction, with triazabicyclodecene (TBD) catalyst, was utilized in the depolymerization (see ¹H NMR under Fig. S7). In quest for a greener depolymerization protocol, we also explored the possibility to replace toluene with a greener solvent, such as p-cymene (Alder et al., 2016), which is recommended by the GSK solvent sustainability guide (Table S11). NMR analysis (Fig. S8) revealed that both toluene and p-cymene were equally suitable as solvents for the depolymerization of P(4,5-T6GBL) into 4,5-T6GBL using TBD organocatalyst. Note that the smaller the size and lower the complexity of an organocatalyst, as in the case of TBD, the more sustainable the catalyst is (Antenucci et al., 2021). Besides, the direct recovery of the monomers, aliphatic polyesters are commonly considered environmentally friendly, because they are enzymatically biodegradable (He et al., 2005).

A phase inversion process was used to convert the polymer into a nanofiltration membrane. Various common and green solvents were explored to prepare a polymer dope solution with a viscosity suitable for membrane fabrication. P(4,5-T6GBL) displayed high solubility in many solvents, such as ethyl acetate, γ -butyrolactone, γ -valerolactone, dimethylformamide (DMF), dimethylacetamide (DMAc), and dimethyl sulfoxide (DMSO), resulting in a low viscosity solution. To improve the viscosity while maintaining a relatively low (25-30 wt.%) dope solution concentration, a more viscous green solvent, PolarClean (viscosity = 7.2 mPa•s), was selected for membrane fabrication. Dissolving P(4,5-T6GBL) in PolarClean at 30 wt.% produced a dope solution with a viscosity of 503 mPa·s, which was adequate for membrane casting. PolarClean, considered a nontoxic replacement for common polar aprotic solvents, which can be derived through green synthesis (Cseri and Szekely, 2019). It can also be synthesized from waste products (Ferlin et al., 2019), and it has been recently used in membrane fabrication (Marino et al., 2018; Ursino et al., 2020; Wang et al., 2019; Xie et al., 2020). The comparison of toxicology, hazardousness, and environmental consideration of PolarClean and other organic solvents are provided in Table S12. Because the polymer was insoluble in water, the cast polymer film was immersed in a coagulation bath of water as the non-solvent.

During phase inversion processes, the chemical structures of polymers are not altered; however, membrane pore structure and surface roughness can be affected. The membrane morphology can change because of differences in solvent and non-solvent diffusivities and evaporation times (Saljoughi et al., 2010). In the current work, we opted to investigate the effect of casting film thickness and solvent/non-solvent diffusivity on the membrane morphology.

To examine the effect of casting film thickness, 30 wt.% P(4,5-T6GBL) dope solution using PolarClean was cast with 250 and 150 μm , and the obtained membranes were denoted as M1 and M2, respectively. The films were subsequently immersed in a water coagulation bath at room temperature (23 °C). The effect of solvent/non-solvent diffusivity was investigated by immersing another 150 μm cast film in a water coagulation bath at an elevated temperature (60 °C), denoted as M3. The morphologies of the fabricated membranes are presented in Fig. 2.

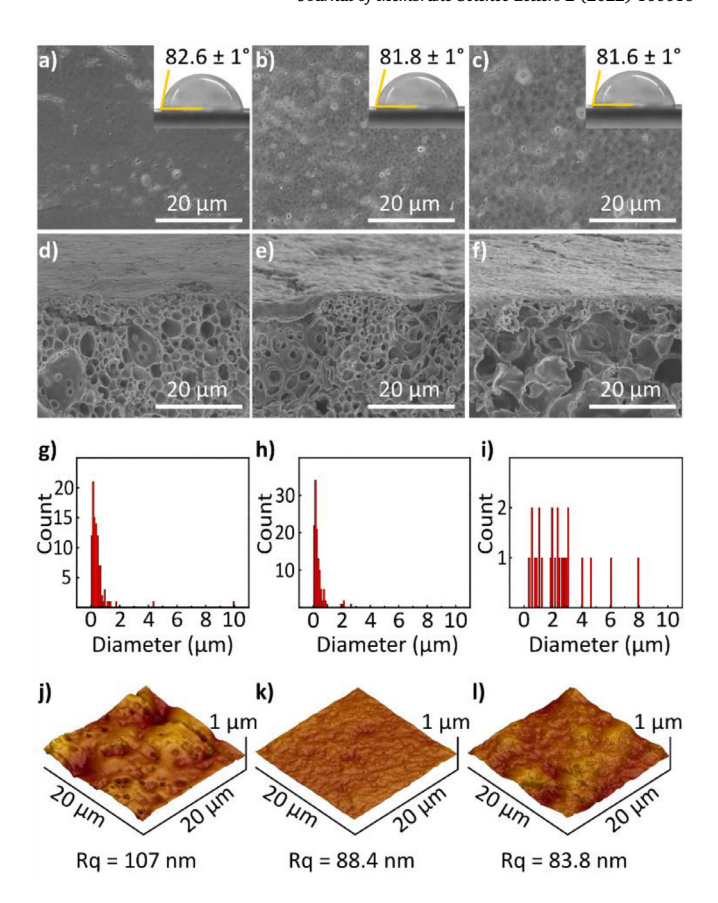


Fig. 2. Morphologies of the P(4,5-T6GBL) membranes. (a–c) SEM surface images of M1, M2, and M3. The insets are the corresponding contact angles. (d–f) Cross-section images of M1, M2, and M3. (g–i) Macrovoid size distributions in the cross-sectional membranes of M1, M2, and M3. (j–l) AFM images and corresponding roughness values (Rq) for M1, M2, and M3.

All membrane surfaces exhibited similar and relatively smooth and homogenous structures (Fig. 2a-c). Notably, some defect formation was unavoidable when drying the SEM samples. The membranes' water contact angles were similar at approx. 82°, providing an additional validation to FTIR (Fig. S1) that the chemical structure of the polymer remained unaffected by the different membrane fabrication conditions (e.g., knife thickness and temperature). Varying the knife thickness during membrane casting did not affect the chemical structure of the polymer and the fabricated membranes, because the process did not involve any chemical treatment, performed at room temperature, and did not involve harsh mechanical protocols. Similarly, increasing the coagulation bath temperature up to 60 °C did not alter the chemical structure of the polymer and the fabricated membrane because the polymer exhibits good thermal stability with a degradation temperature of 317 °C (Fig. 1e) and glass transition temperature of 72.7 °C (Fig. S3). The obtained medium value for the contact angle was attributed to the presence of both hydrophobic aliphatic cyclohexane rings and hydrophilic ester groups in the polymer framework. The membranes had a spongelike macrovoid structure, as observed in the scanning electron microscopy (SEM) cross-section images (Fig. 2d-f). The structure and size of the macrovoids in M1 and M2 were similar, with equally narrow dimensions; the mean macrovoid width was approx. 0.15 µm (Fig. 2g and h), and in both cases, the macrovoids were quasi circular. The similar shape of the M1 and M2 cross-section morphologies indicated that membrane thickness did not influence the formation of the cross-sectional structure. The thicknesses of M1, M2, and M3 were 138 ± 4 , 73 ± 3 , and 77 ± 3 µm, respectively (Fig. S2), and the M3 cross-section appeared to be differ-

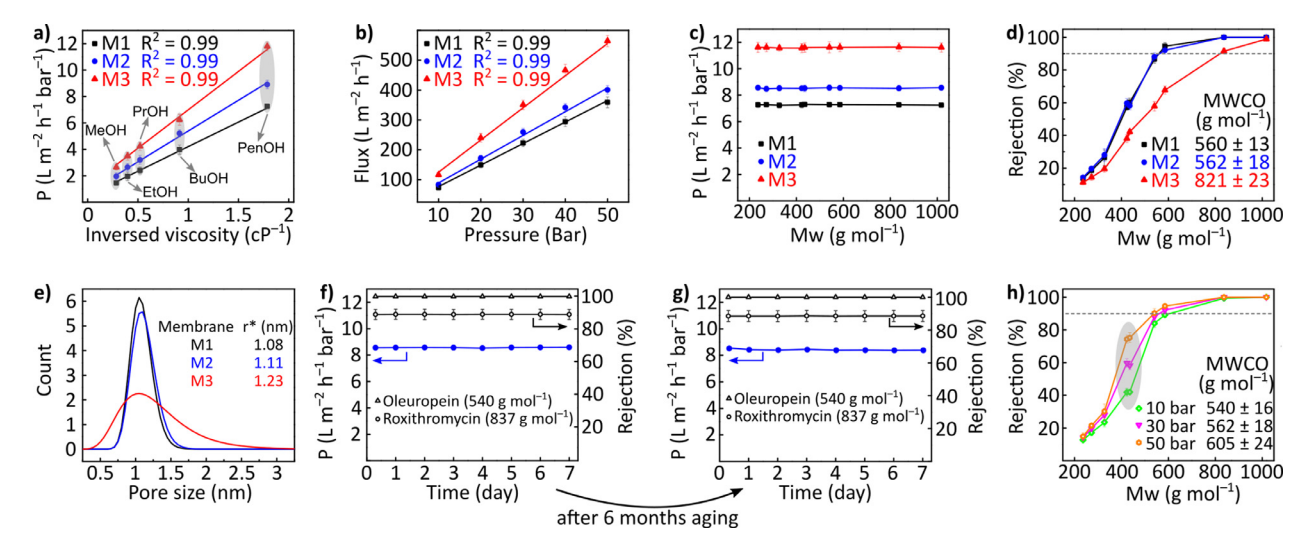


Fig. 3. Nanofiltration performance of M1 (250 μ m, 23 °C), M2 (150 μ m, 23 °C), and M3 (150 μ m, 60 °C). (a) Permeance vs. solvent viscosity, (b) flux as a function of applied pressure, (c) influence of solute on permeance, (d) rejection profile of various dyes and pharmaceutical molecules, (e) pore size distribution, (f) long-term stability test of freshly prepared M2, (g) long-term stability test of M2 after 6 months aging, and (h) effect of pressure on the rejection profile of M2. All data were obtained in methanol at 30 bar unless otherwise stated.

ent, with a less regular shape and a wider range of mean macrovoid sizes (Fig. 2f and i). This clearly indicated the effect of the coagulation bath temperature on the formation of the macrovoid structure across the membrane. Additionally, AFM analysis showed that the thicker M1 membrane had a rougher surface than its thinner M2 counterpart (compare Fig. 2j and k). However, the results indicated that the coagulation bath temperature did not affect the membrane surface roughness (compare Fig. 2k and l).

The formation of the more open macrovoid structure at a higher coagulation bath temperature was attributed to altered diffusion. When the cast polymer film was immersed in a coagulation bath, the miscibility of the solvent (PolarClean) and the non-solvent (water) caused diffusional flow (i.e., exchange of the solvent and non-solvent), and phase separation occurred. Polymer precipitation started simultaneously because of the low solubility of the polymer in the non-solvent (water). This process resulted in the formation of an integrally skinned asymmetric (ISA) membrane with a dense top layer (i.e., a thin skin layer) and a porous sublayer. The formation of phase-inversion membranes is influenced by both thermodynamic factors, related to the phase equilibrium between components in the coagulation bath, and kinetic factors, related to their mutual diffusivities (Saljoughi et al., 2010). Increasing the temperature from 23 °C to 60 °C interrupted the phase equilibrium and increased the mutual diffusivities, which resulted in the rapid demixing of the water and the PolarClean (i.e., the rapid formation of M3 in the coagulation bath). This instantaneous demixing created a more open structure (Saljoughi et al., 2010): the formation of macrovoids occurred under rapid precipitation conditions and the precipitation was quicker at higher temperatures. This observation is in accordance with the reported literature on the effects of coagulation bath temperature on membrane morphology (Saljoughi et al., 2010).

The separation performance of the membranes was evaluated for OSN. The stability test on the fabricated membranes revealed that these membranes were stable in various alcohols and aqueous media. However, the membranes dissolved in other organic solvents such as acetone, toluene, hexane, and DMF. The membranes exhibited excellent stability in alcohols, and the M1, M2, and M3 permeances for various alcohols were determined (Fig. 3a). Permeance was observed to be inversely proportional to solvent viscosity. Owing to its overall low resistance, the thinner M2 membrane exhibited higher permeance compared to the thicker M1 membrane. M3, which had a similar membrane thickness to M2, exhibited the highest permeance owing to its more open

cross-sectional macrovoid structure (see Fig. 2f), which had less material resistance. The relationship between permeance with other solvent properties, such as polarity, molecular volume, and density were also evaluated (Fig. S6). Despite no obvious correlation was observed between the polarity, density and the solvent permeance, a decrease in permeance as a function of molecular volume of the solvents was observed (Fig. S6b). This phenomenon can be explained by the fact that larger solvent molecules are more resistant to transport through the membrane, which resulted in lower permeance. The solvent flux linearly increased as a function of the applied pressure (Fig. 3b).

To assess the molecular sieving properties of the membranes, nine solutes, having molecular weights between 200 and 1000 g mol⁻¹ were filtered under cross-flow conditions at 30 bar (Fig. 3d). The methanol permeance of all the membranes was independent of the chemical nature and size of the solute (Fig. 3c). M1 and M2 showed virtually the same rejection profiles with molecular weight cut-offs (MWCOs) of 560 $\pm\,13$ and $562 \pm 18 \text{ g mol}^{-1}$, respectively, whereas M3 had a different rejection profile with a higher MWCO of 821 ± 23 g mol⁻¹. The similar M1 and M2 rejection profiles indicated that the thickness did not affect the membrane skin layer responsible for the solute rejection. In contrast, a higher coagulation bath temperature (M3) opened the skin layer considerably at the molecular level, allowing larger solutes to pass through the membrane. A similar trend has been previously reported in the literature (Xu et al., 2014). M1 and M2 exhibited similar pore size distribution profile with a mean pore size of 1.08 and 1.11 nm, respectively. A broader pore size distribution was observed in M3 with a larger mean pore size of 1.23 nm (Fig. 3e).

Long-term membrane stability was tested in a continuous crow-flow filtration rig over a week (Fig. 3f). The methanol permeance was stable at $8.6 \pm 0.1~L~m^{-2}~h^{-1}~bar^{-1}$, and the rejection profiles of the pharmaceuticals oleuropein (540 g mol^-1) and roxithromycin (837 g mol^-1) were also stable at 87% and 100%, respectively. Stable steady-state performance was observed over a seven-days-long continuous filtration, which suggests that there is neither significant compaction nor fouling on the membrane. The long-term membrane stability was maintained when re-testing the same membrane after it has been stored in the filtration solvent and cell over 6 months (Fig. 3g). These results suggest negligible aging and indicated that the polymer chains were not rearranged under the applied conditions. Moreover, the cross-flow filtration helped to wash away the possible foulants and minimized concentration-polarization. The effect of applied pressure on the rejection profile is

presented in Fig. 3h. Increasing the applied pressure during the OSN test did not significantly change the rejection of solutes with molecular weights less than approx. 350 mol⁻¹ and greater than approx. 550 g mol⁻¹. The MWCO slightly increased as the pressure was increased. However, the observed rejection values of valsartan and losartan (approx. 430 g mol⁻¹) pharmaceutical solutes were considerably increased with an increase in pressure: 40% at 10 bar, 60% at 30 bar, and 80% at 50 bar. Note that these solutes fell close to the inflection point of the MWCO curve in Fig. 3h. The selectivity of the membranes was easily altered with respect to solutes with medium rejection values, whereas solutes having particularly low or high rejections were less prone to change. These results demonstrated that molecular sieving performance can be fine-tuned in the range of approx. 350 to 550 g mol⁻¹, by controlling the applied pressure. In general, solute rejection is expected to increase with increasing pressure due to the preferential enhancement in solvent flux (solution-diffusion mechanism).

4. Conclusion

In summary, we successfully used a biosourced polyester, P(4,5-T6GBL), to fabricate a nanofiltration membrane using PolarClean, a green solvent. The polymer is chemically recyclable to a monomer. The membrane exhibited strong resistance toward alcohols and demonstrated tunable nanofiltration performance. The M1 and M2 membranes exhibited quasi-complete rejection toward solutes with molecular weights greater than 600 g mol⁻¹, and their approximate MWCOs were quasi identical (561 g mol⁻¹). M2 also exhibited excellent long-term stability under continuous cross-flow filtration over one week. The development of fully recyclable polymer membranes offers a sustainable alternative to more complex and nonrecyclable linear, branched, and crosslinked polymer membrane architectures. All aspects of this research, including the monomer source, polymer synthesis method, membrane fabrication, application, and polymer recyclability, were in accordance with sustainability and circular economy principles.

Statement of novelty

The majority of OSN membrane fabrication still relies on petrochemical derivatives as raw materials and processed using toxic, harmful, and unsustainable solvents. Moreover, end-of-life and recyclability issues of the fabricated membranes are yet to be fully explored and resolved. Herein, for the first time, we have developed OSN membranes based on biosourced and fully recyclable polyester, P(4,5-T6GBL), using PolarClean, an emerging green solvent. The polymer was obtained by sustainably transforming renewable monomers via organocatalysis (which is more environmentally friendly than metal-based catalysis) under ambient conditions. This polyester can be chemically depolymerized, which potentially provides a way out of the unsustainable end-of-use incineration of membranes and offers a closed-loop approach toward a circular materials economy.

Declaration of Competing Interest

The authors declare that they have no known competing financial interests or personal relationships that could have appeared to influence the work reported in this paper.

Acknowledgements

The research reported in this publication was supported by funding provided by the King Abdullah University of Science and Technology (KAUST), and the US National Science Foundation (NSF-1955482). We thank Mahmoud Abdulhamid for the assistance with the NMR analysis.

Supplementary materials

Supplementary material associated with this article can be found, in the online version, at doi:10.1016/j.memlet.2022.100016.

References

- Alder, C.M., Hayler, J.D., Henderson, R.K., Redman, A.M., Shukla, L., Shuster, L.E., Sneddon, H.F., 2016. Updating and further expanding GSK's solvent sustainability guide. Green Chem. 18, 3879–3890. doi:10.1039/C6GC00611F.
- Antenucci, A., Dughera, S., Renzi, P., 2021. Green chemistry meets asymmetric organocatalysis: a critical overview on catalysts synthesis. ChemSusChem 14, 2785– 2853. doi:10.1002/cssc.202100573.
- Caretto, A., Noè, M., Selva, M., Perosa, A., 2014. Upgrading of biobased lactones with dialkylcarbonates. ACS Sustain. Chem. Eng. 2, 2131–2141. doi:10.1021/sc500323a.
- Cseri, L., Szekely, G., 2019. Towards cleaner PolarClean: efficient synthesis and extended applications of the polar aprotic solvent methyl 5-(dimethylamino)-2-methyl-5-oxopentanoate. Green Chem. 21, 4178–4188. doi:10.1039/C9GC01958H.
- Cywar, R.M., Zhu, J.-B., Chen, E.Y.-X., 2019. Selective or living organopolymerization of a six-five bicyclic lactone to produce fully recyclable polyesters. Polym. Chem. 10, 3097–3106. doi:10.1039/C9PY00190E.
- Ferlin, F., Luciani, L., Viteritti, O., Brunori, F., Piermatti, O., Santoro, S., Vaccaro, L., 2019. Polarclean as a sustainable reaction medium for the waste minimized synthesis of heterocyclic compounds. Front. Chem 6, 659. doi:10.3389/fchem.2018.00659.
- Figoli, A., Marino, T., Simone, S., Nicolò, E.D., Li, X.-M., He, T., Tornaghi, S., Drioli, E., 2014. Towards non-toxic solvents for membrane preparation: a review. Green Chem. 16. 4034–4059. doi:10.1039/C4GC00613E.
- Goh, K.S., Chen, Y., Chong, J.Y., Bae, T.H., Wang, R., 2021. Thin film composite hollow fibre membrane for pharmaceutical concentration and solvent recovery. J. Membr. Sci. 621, 119008. doi:10.1016/j.memsci.2020.119008.
- He, F., Li, S., Garreau, H., Vert, M., Zhuo, R., 2005. Enzyme-catalyzed polymerization and degradation of copolyesters of ε-caprolactone and γ-butyrolactone. Polymer 46, 12682–12688. doi:10.1016/j.polymer.2005.10.121.
- Hessel, V., Tran, N.N., Asrami, M.R., Tran, Q.D., Long, N.V.D., Escribà-Gelonch, M., Tejada, J.O., Linke, S., Sundmacher, K., 2022. Sustainability of green solvents review and perspective. Green Chem. doi:10.1039/D1GC03662A, In press.
- Hong, M., Chen, E.Y.-X., 2016. Towards truly sustainable polymers: a metal-free recyclable polyester from biorenewable non-strained γ-butyrolactone. Angew. Chem. Int. Ed. 55, 4188–4193. doi:10.1002/anie.201601092.
- Jagatić Korenika, A.-M., Preiner, D., Tomaz, I., Jeromel, A., 2020. Volatile profile characterization of croatian commercial sparkling wines. Molecules 25, 4349. doi:10.3390/molecules25184349.
- Kim, D., Nunes, S.P., 2021. Green solvents for membrane manufacture: recent trends and perspectives. Curr. Opin. Green Sustain Chem. 28, 100427. doi:10.1016/j.cogsc.2020.100427.
- Marchetti, P., Jimenez Solomon, M.F., Szekely, G., Livingston, A.G., 2014. Molecular separation with organic solvent nanofiltration: a critical review. Chem. Rev. 114, 10735–10806. doi:10.1021/cr500006i.
- Marino, T., Blasi, E., Tornaghi, S., Di Nicolò, E., Figoli, A., 2018. Polyethersulfone membranes prepared with Rhodiasolv®Polarclean as water soluble green solvent. J. Membr. Sci. 549, 192–204. doi:10.1016/j.memsci.2017.12.007.
- McKeown, P., Kamran, M., Davidson, M.G., Jones, M.D., Román-Ramírez, L.A., Wood, J., 2020. Organocatalysis for versatile polymer degradation. Green Chem. 22, 3721– 3726. doi:10.1039/D0GC01252A.
- Saljoughi, E., Amirilargani, M., Mohammadi, T., 2010. Effect of PEG additive and coagulation bath temperature on the morphology, permeability and thermal/chemical stability of asymmetric CA membranes. Desalination 262, 72–78. doi:10.1016/j.desal.2010.05.046.
- Ursino, C., Russo, F., Ferrari, R.M., De Santo, M.P., Di Nicolò, E., He, T., Galiano, F., Figoli, A., 2020. Polyethersulfone hollow fiber membranes prepared with Polarclean® as a more sustainable solvent. J. Membr. Sci. 608, 118216. doi:10.1016/j.memsci.2020.118216.
- Wang, H.H., Jung, J.T., Kim, J.F., Kim, S., Drioli, E., Lee, Y.M., 2019. A novel green solvent alternative for polymeric membrane preparation via nonsolvent-induced phase separation (NIPS). J. Membr. Sci. 574, 44–54. doi:10.1016/j.memsci.2018.12.051.
- Winkler, M., Romain, C., Meier, M.A.R., Williams, C.K., 2014. Renewable polycarbonates and polyesters from 1,4-cyclohexadiene. Green Chem. 17, 300–306. doi:10.1039/C4GC01353K.
- Xie, W., Li, T., Tiraferri, A., Drioli, E., Figoli, A., Crittenden, J.C., Liu, B., 2021. Toward the next generation of sustainable membranes from green chemistry principles. ACS Sustain. Chem. Eng. 9, 50–75. doi:10.1021/acssuschemeng.0c07119.
- Xie, W., Tiraferri, A., Liu, B., Tang, P., Wang, F., Chen, S., Figoli, A., Chu, L.-Y., 2020. First Exploration on a poly(vinyl chloride) ultrafiltration membrane prepared by using the sustainable green solvent polarclean. ACS Sustain. Chem. Eng. 8, 91–101. doi:10.1021/acssuschemeng.9b04287.
- Xu, J., Tang, Y., Wang, Y., Shan, B., Yu, L., Gao, C., 2014. Effect of coagulation bath conditions on the morphology and performance of PSf membrane blended with a capsaicin-mimic copolymer. J. Membr. Sci. 455, 121–130. doi:10.1016/j.memsci.2013.12.076.
- Zhu, J.-B., Chen, E.Y.-X., 2018. Living coordination polymerization of a six-five bicyclic lactone to produce completely recyclable polyester. Angew. Chem. Int. Ed. 57, 12558– 12562. doi:10.1002/anie.201808003.

Zhu, J.-B., Watson, E.M., Tang, J., Chen, E.Y.-X., 2018. A synthetic polymer system with repeatable chemical recyclability. Science 360, 398–403. doi:10.1126/science.aar5498.

Zou, D., Nunes, S.P., Vankelecom, I.F.J., Figoli, A., Lee, Y.M., 2021. Recent advances in polymer membranes employing non-toxic solvents and materials. Green Chem. 23, 9815–9843. doi:10.1039/D1GC03318B.